Chapter 6
High-Speed Trains with Different Tracks on Layered Ground and Measures to Increase Critical Speed

Amir M. Kaynia

6.1 Introduction

6.1.1 Early Studies on Moving Loads

The early studies in the field of moving loads on elastic media date back to the middle of the nineteenth century; however, interest in the theoretical solutions appears to have been triggered by Sneddon in 1951. Since then, numerous solutions with different constraints and varying degrees of sophistication have been reported in the literature. The complexity of the problem has largely confined the solutions to loads moving on homogeneous elastic half-space solids. The existing solutions can be broadly divided into 2D and 3D solutions. An important differentiation between the various solutions has been the range of load speeds. This is because the form of the solution depends primarily on the speed of the load with respect to the characteristic wave velocities of the propagating medium. It is common to refer to load speed as sub-seismic, super-seismic and trans-seismic, depending on whether the load speed is less than the Rayleigh wave velocity of the medium, greater than the longitudinal wave velocity or intermediate between those two velocities (Baron et al. 1967). The speed corresponding to the Rayleigh wave velocity is often called the *critical speed* (e.g., Madshus and Kaynia 2000), because below this speed, the ground response is primarily quasi-static, whereas for higher speeds, the ground response is largely characterized by dynamic features and larger magnitudes.

Two-dimensional solutions, i.e., solutions for a moving line load, have been presented by Sneddon (1951), Cole and Huth (1958), Ang (1960), Craggs (1960), Payton (1964), Eringen and Suhubi (1975). Sneddon developed a closed-form

A. M. Kaynia (✉)
Norwegian Geotechnical Institute (NGI), Oslo, Norway
e-mail: amir.m.kaynia@ngi.no; amir.kaynia@ntnu.no

A. M. Kaynia
Norwegian University of Science and Technology (NTNU), Trondheim, Norway

T. G. Sitharam et al. (eds.), *Latest Developments in Geotechnical Earthquake Engineering and Soil Dynamics*, Springer Transactions in Civil and Environmental Engineering, https://doi.org/10.1007/978-981-16-1468-2_6

solution using integral transforms; however, he focused his attention to the case of low speeds. Cole and Huth (1958) investigated the same problem and considered the trans-seismic and super-seismic speeds, as well. They used the Helmholtz decomposition technique to decouple the shear and compressional wave components, solved the resulting equations using the techniques of complex analytic functions and derived closed-form expressions for the displacements and stresses in a half-space. They defined Mach numbers $M_P = C_P/V$ and $M_S = C_S/V$ to represent the speed of the moving load, V, relative to the pressure wave velocity, C_P and shear wave velocity, C_S, of the medium. Eringen and Suhubi (1975) followed the same solution scheme and presented results for the trans-seismic and super-seismic speeds in addition to duplicating the Cole and Huth (1958) results for the sub-seismic load speed.

Other relevant 2D solutions are due to Ang (1960), Papadopoulos (1963) and Niwa and Kobayashi (1966) who used the Helmholtz decomposition technique to uncouple the dilatational (pressure) and distortional (shear) components. Ang [1] solved the equations for the sub-seismic case by using the Laplace transform and the Laplace inversions by a numerical technique, whereas Niwa and Kobayashi (1966) used the Fourier transform. A detailed review of the early studies on the subject can be found in Frýba (1973).

For layered half-space, the only analytical solutions appear to have been advanced by Sackman (1961) and Wright and Baron (1970). Sackman (1961) used for each layer the solutions for the dilatational and distortional potentials obtained by Cole and Huth (1958) and constructed the wave field from multiple reflections and refractions of plane waves from plane boundaries. Wright and Baron (1970) considered a soil layer over a half-space under a moving pressure pulse with a speed which is super-seismic with respect to the surficial layer and sub-seismic with respect to the half-space. They used the potential theory combined with the Fourier transform along the horizontal axis and derived formal integral solutions for stresses and velocities, which they in turn solved numerically. In this context, Achenbach et al. (1967) used the potential approach and by numerically evaluating the integrals studied the response of a plate, resting on a half-space, to a moving line load. Although they only considered the sub-seismic case, they were able to document large bending moments in the plate as the load speed approached the Rayleigh wave velocity in the half-space.

For general heterogeneous soil, researchers have had to resort to semi-analytical or purely numerical solutions. Several different semi-analytical models have been developed for this problem. These models consider the load either moving on a plate or track over a half-space (e.g., Pan and Atluri 1995; Krylov 1995), or directly moving over a layered half-space (e.g., Aubry et al. 1994; de Barros and Luco 1994). Krylov (1995) investigated the problem of a train moving on a track with sleeper periodicity d. He used a classical beam-on-elastic-foundation solution and calculated the contribution of each sleeper to the total pressure distribution. Then, by assuming each sleeper as a point source and convolving its pressure distribution by the half-space Green's functions, he derived formal solutions for the vertical component of the ground surface motions. He used, however, only the Rayleigh

wave contribution to the Green's functions. Results of Krylov's model agree with theoretical solutions. More specifically, his results show the formation of Mach lines with accurate Mach angles for the trans-seismic speed and show that no radiation wave fields exist for speeds less than the Rayleigh wave velocity of the medium.

One of the most rigorous formulations and extensive numerical results has been presented by de Barros and Luco (1994). They developed a semi-analytical formulation for the ground vibrations due to a point load moving on or inside a layered viscoelastic half-space. The frequency-domain formulation of de Barros and Luco (1994) is based on double Fourier transform in the two horizontal spatial coordinates. For each layer, the transformed displacements and stresses at the layer boundaries were expressed in terms of the wave amplitudes in that layer through the so-called transmission and reflection matrices. The wave amplitudes were obtained by imposition of the appropriate condition at the layer interfaces. The inversion of the Fourier integrals from the wave number domain to the space domain was achieved by a quadrature algorithm (Filon 1928), and the response in the time domain was obtained through the inverse Fourier transform.

6.1.2 Studies on High-Speed Trains

The development of high-speed trains and their increased deployment in areas with low shear wave velocities, which bring the train speeds closer to the trans-seismic regime, has stimulated an extensive research on the subject since the 1990s. The solutions described above have inspired a host of new semi-empirical and numerical solutions and applications. They vary from 2D finite element solutions (e.g., Peplow and Kaynia 2007; Norén-Cosgriff et al. 2019) to 3D finite element (e.g., Hall 2003), combination of finite element and boundary element solutions (e.g., Andersen and Jones 2006 and Auersch 2005) and 2.5-D schemes (e.g., Coulier et al. 2013). The latter approach allows reducing the computational demand in models where the track is considered as invariant in the direction of the load passage. This allows the problem to be described with a 2D geometry while the loading is accounted for in 3D. This approach can also be combined with the boundary element method resulting in computationally efficient models (e.g., Karlström and Boström 2006).

An alternative solution is an efficient analytical–numerical 3D solution by use of the sub-structuring technique. In this solution, the dynamic response of the layered ground is represented by Green's functions, and the track is represented by finite elements (e.g., Kaynia et al. 2000). Two versions of this model are used in the present study. The next section presents the principles of these models, and the subsequent sections provide representative results of simulations for both models and the features of the responses. The main objective of this study is to investigate how to increase the critical speed in order to avoid excessive track responses associated with trans-seismic and super-seismic conditions.

6.2 Simulation Models

6.2.1 Track Cases

Two track concepts were considered in the present study. The first one is the conventional tracks consisting of the rail/ballast/sub-ballast placed either directly over the ground or over an embankment. This case is referred to as *surface track* in this study and is shown in Fig. 6.1a. For this case, two solutions for increasing the critical speed were considered: (1) stiffened track and (2) ground treatment, for example by replacing part of the natural soil by stiffer material or by grouting (Fig. 6.1c).

The second track concept consisted of the rail/ballast/sub-ballast placed on a deck (beam) resting on large-diameter piles. This case, which resembles a bridge, is portrayed in Fig. 6.2 and is referred to as *piled track*. While the deck could be initially in contact with the ground, the contact is weakened or possibly lost with time. This case can in practice be considered as a measure to increase the critical speed the same way that the soil improvement/replacement in Fig. 6.1c is considered.

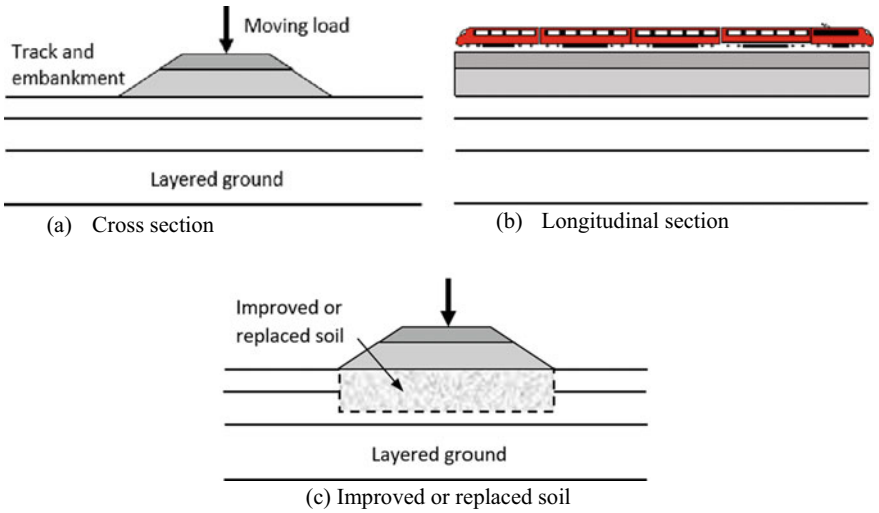

Fig. 6.1 Key features of surface track on layered ground: **a** cross section with idealized train load, **b** longitudinal section with schematics of train cars and **c** track with soil improvement or replacement

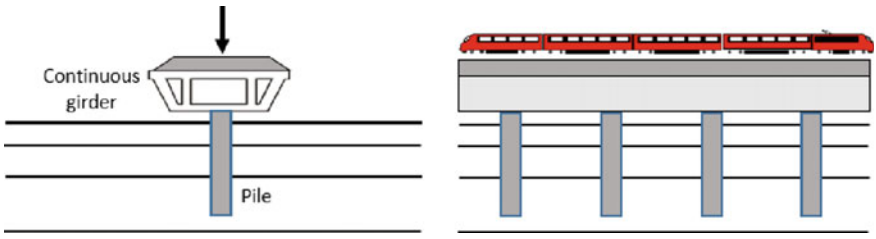

(a) Cross section (b) Longitudinal section

Fig. 6.2 Key features of piled track on layered ground: **a** cross section with idealized train load and **b** longitudinal section with piles and schematics of train cars

6.2.2 Computational Tools

For the surface track cases in Fig. 6.1, the numerical simulation tool *VibTrain* (Kaynia et al. 2000) was used. For the piled track concept in Fig. 6.2, the numerical model *VibTrain_pile*, which was recently developed by the author, was employed. A brief account of these models is presented in the following.

The solutions of both cases are based on sub-structuring in which the ground or the piles in the second track concept are represented by the impedance matrices at the track–support interface. For the surface track model, the interface nodes are defined by regularly placed points along the track. For the piled track concept, the interface nodes are the pile heads. If the vertical displacements and forces at these nodes are denoted by $\boldsymbol{W}$ and $\boldsymbol{P}$, one can write

$$\boldsymbol{P} = \boldsymbol{G}^{-1}\boldsymbol{W} = \boldsymbol{K}_S\boldsymbol{W} \tag{6.1}$$

where $\boldsymbol{K}_S$ is the impedance matrix of the ground nodes (or pile heads in the piled track model). A similar relationship can be established by considering the equilibrium of the track sub-structure as

$$\boldsymbol{F} - \boldsymbol{P} = \boldsymbol{K}_B\boldsymbol{W} \tag{6.2}$$

where $\boldsymbol{F}$ is the vector of applied nodal loads (i.e., moving loads) and $\boldsymbol{K}_B$ is the dynamic stiffness matrix of the track. Elimination of the interaction force vector, $\boldsymbol{P}$, from Eqs. (6.1) and (6.2) leads to following equations of the coupled system.

$$\boldsymbol{F} = (\boldsymbol{K}_B + \boldsymbol{K}_S)\boldsymbol{W} \tag{6.3}$$

By taking the Fourier transform of the applied loads, solving Eq. (6.3) for the Fourier frequencies, and combining the frequency contributions by the inverse Fourier transform, one can compute the time histories of the track response. See Kaynia et al. (2000) for details. This formulation was extended to cases where the excitation is due to rail roughness by Kaynia (2001) and to cases involving track defects, such as hanging sleepers, by Kaynia et al. (2017).

For computation of the ground impedance and pile impedance matrices, one needs the Green's functions of the layered soil for unit loads on the ground surface in the first model and the Green's functions for cylindrical loads representing pile–soil tractions in the second model. These functions are described in the following sections.

6.2.3 Green's Functions for Layered Viscoelastic Soil

Park and Kaynia (2018) recently developed a semi-analytical solution for the Green's functions for unit disk loads and pressure sources in layered anisotropic layered ground under water. The solution is an extension of the model proposed by Kausel and Roesset (1981) for isotropic soil media. The solution technique is based on the application of Fourier and Hankel transforms to the wave equations in each layer to reduce them to a series of ordinary differential equations. These equations are then solved by the imposition of the appropriate stress and kinematic boundary conditions at layer interfaces and the free surface. This is achieved through a stiffness matrix approach in which each layer is represented by a stiffness matrix that relates the Fourier transform of the stresses and displacements at the upper and lower surfaces of the layer. Stiffness expressions derived by Park and Kaynia (2018) are incorporated here for completeness. The reader is referred to the original reference for the details.

If λ_t and G_t are the complex *Lamé* constants related to wave motion propagating in the vertical direction (z), and λ and G are related to wave propagation in the two horizontal directions (r,θ), then the associated wave velocities can be expressed by

$$C_p = \sqrt{\frac{\lambda + 2G}{\rho}};\quad C_s = \sqrt{\frac{G}{\rho}};\quad C_{pt} = \sqrt{\frac{\lambda_t + 2G_t}{\rho}};\quad C_{st} = \sqrt{\frac{G_t}{\rho}} \tag{6.4}$$

where ρ is the mass density, C_p and C_s are the P- and S-wave velocities in x-y plane (i.e., along the horizontal direction); C_{pt} and C_{st} are the corresponding velocities in the vertical direction. The anisotropy can be defined by introducing the following three parameters defining the ratios between these wave velocities.

$$\alpha = \frac{C_{pt}}{C_{st}};\quad a = \frac{C_p}{C_{pt}};\quad b = \frac{C_s}{C_{st}} \tag{6.5}$$

The 4×4 stiffness matrix for an anisotropic soil layer subjected to P-SV wave motion is given by the following formula.

$$\mathbf{K} = 2kG_t \begin{Bmatrix} \mathbf{K}_{11} & \mathbf{K}_{12} \\ \mathbf{K}_{21} & \mathbf{K}_{22} \end{Bmatrix} \tag{6.6}$$

where the sub-matrices in the above formula are given by

$$\mathbf{K}_{11} = \frac{\left(\bar{k}_{z1}/\gamma_1 - \bar{k}_{z2}/\gamma_2\right)}{2D_t}\left\{\begin{array}{cc} \gamma_2\left(C_1S_2 - \frac{\gamma_1}{\gamma_2}C_2S_1\right) & -\left[(1-C_1C_2) + \frac{\gamma_1}{\gamma_2}S_1S_2\right] \\ -\left[(1-C_1C_2) + \frac{\gamma_1}{\gamma_2}S_1S_2\right] & \frac{1}{\gamma_1}\left(C_2S_1 - \frac{\gamma_1}{\gamma_2}C_1S_2\right) \end{array}\right\}$$
$$-\frac{1}{2}\left(1+\bar{k}_{z2}/\gamma_2\right)\left\{\begin{array}{cc} 0 & 1 \\ 1 & 0 \end{array}\right\}$$
$$\mathbf{K}_{12} = \frac{\left(\bar{k}_{z1}/\gamma_1 - \bar{k}_{z2}/\gamma_2\right)}{2D_t}\left\{\begin{array}{cc} \gamma_2\left(\frac{\gamma_1}{\gamma_2}S_1 - S_2\right) & -(C_1 - C_2) \\ (C_1 - C_2) & \frac{1}{\gamma_1}\left(\frac{\gamma_1}{\gamma_2}S_2 - S_1\right) \end{array}\right\} = \mathbf{K}_{21}^T$$
$$\mathbf{K}_{22} = \frac{\left(\bar{k}_{z1}/\gamma_1 - \bar{k}_{z2}/\gamma_2\right)}{2D_t}\left\{\begin{array}{cc} \gamma_2\left(C_1S_2 - \frac{\gamma_1}{\gamma_2}C_2S_1\right) & \left[(1-C_1C_2) + \frac{\gamma_1}{\gamma_2}S_1S_2\right] \\ \left[(1-C_1C_2) + \frac{\gamma_1}{\gamma_2}S_1S_2\right] & \frac{1}{\gamma_1}\left(C_2S_1 - \frac{\gamma_1}{\gamma_2}C_1S_2\right) \end{array}\right\}$$
$$+\frac{1}{2}\left(1+\bar{k}_{z2}/\gamma_2\right)\left\{\begin{array}{cc} 0 & 1 \\ 1 & 0 \end{array}\right\} \tag{6.7}$$

The 2 × 2 stiffness matrix for an anisotropic half-space subjected to P-SV wave is expressed as

$$\mathbf{K}_{\text{half}} = 2kG_t\left[\frac{\left(\bar{k}_{z1}/\gamma_1 - \bar{k}_{z2}/\gamma_2\right)}{2(1-\gamma_1/\gamma_2)}\left\{\begin{array}{cc} \gamma_1 & 1 \\ 1 & 1/\gamma_2 \end{array}\right\} - \frac{1}{2}\left(1+\bar{k}_{z1}/\gamma_1\right)\left\{\begin{array}{cc} 0 & 1 \\ 1 & 0 \end{array}\right\}\right] \tag{6.8}$$

Similarly, the stiffness matrices for an anisotropic layer and a half-space subjected to SH were derived and are defined as

$$\mathbf{K} = kG_t\left\{\begin{array}{cc} \mathbf{K}_{11} & \mathbf{K}_{12} \\ \mathbf{K}_{21} & \mathbf{K}_{22} \end{array}\right\} = kG_t\frac{\bar{k}_{z3}}{S_3}\left\{\begin{array}{cc} C_3 & -1 \\ -1 & C_3 \end{array}\right\} \tag{6.9}$$

$$\mathbf{K}_{\text{half}} = kG_t\bar{k}_{z3} \tag{6.10}$$

The parameters in the above formula are defined in the following.

$$C_1 = \cos\, hk\bar{k}_{z1}h,\ S_1 = \sin\, hk\bar{k}_{z1}h \tag{6.11a}$$

$$C_2 = \cos\, hk\bar{k}_{z2}h,\ S_2 = \sin\, hk\bar{k}_{z2}h \tag{6.11b}$$

$$C_3 = \cos\, hk\bar{k}_{z3}h,\ S_3 = \sin\, hk\bar{k}_{z3}h \tag{6.11c}$$

$$D_t = 2(1 - C_1C_2) + \left(\frac{\gamma_1}{\gamma_2} + \frac{\gamma_2}{\gamma_1}\right)S_1S_2 \tag{6.11d}$$

$$\bar{k}_{z1} \text{ or } \bar{k}_{z2} = \sqrt{\frac{\alpha^2(a^2-1)+2-(1+\alpha^{-2})\Omega_{st}^2 \pm \sqrt{\left[\alpha^2(a^2-1)-(1-\alpha^{-2})\Omega_{st}^2\right]^2+4(a^2-1)(\alpha^2-1)}}{2}} \tag{6.11e}$$

$$\bar{k}_{z3} = \sqrt{b^2-\Omega_{st}^2};\ \gamma_1 = \frac{\alpha^2 a^2 - \bar{k}_{z1}^2 - \Omega_{st}^2}{(\alpha^2-1)\bar{k}_{z1}};\ \gamma_2 = \frac{\alpha^2 a^2 - \bar{k}_{z2}^2 - \Omega_{st}^2}{(\alpha^2-1)\bar{k}_{z2}} \tag{6.11f}$$

$$\Omega_{pt} = \frac{\omega}{kC_{pt}} = \frac{\Omega_{st}}{\alpha};\ \Omega_{st} = \frac{\omega}{kC_{st}} \tag{6.11g}$$

As expected, by setting $a = 1$ and $b = 1$ in the above matrices one can recover the stiffness matrices for the isotropic medium developed by Kausel and Roesset (1981).

6.2.4 *Green's Functions for Piles in Layered Soil*

The Green's functions for cylindrical loads, representing pile–soil tractions, are those developed by Kaynia (1988). The solution is based on the stiffness matrix approach and in principle is similar to the one described above. For details, the reader is referred to Kaynia (1988) and Kaynia and Kausel (1991).

6.3 Soil and Load Data and Simulation for Base Case

The numerical results presented in the following sections correspond to the ground conditions established at a test site in Ledsgård, Sweden and for the Swedish passenger train X-2000. The soil at this site was characterized through a series of laboratory and field measurements. The parameters determined for the site for two speed regimes, namely sub-seismic and trans-seismic, were reported in Kaynia et al. (2000) and are summarized in Table 6.1. Figure 6.3 shows the bogie loads for the X-2000 train.

The track (including ballast and embankment) was represented by an equivalent beam with bending rigidity, $EI = 200$ MNm^2 for sub-seismic speed regime and 80 MNm^2 for trans-seismic condition (Kaynia et al. 2000). The different values of soil parameters (also in Table 6.1) reflect the soil nonlinearity. Mass of the track was taken 10,600 kg/m.

Figure 6.4 displays the computed time history of track displacements for the surface track base case (i.e., with no countermeasures) for train passages in different speed regimes, sub-seismic (100 and 140 km/h), critical speed (200 km/h) and trans-seismic (250 km/h). As the plots show, the response in the sub-seismic regime

Table 6.1 Soil parameters at Ledsgård test site used in numerical simulations

Soil layer	Thickness [m]	Density [kg/m^3]	C_S [m/s]		C_P [m/s]	
			V = 70 [km/h]	V = 200 [km/h]	V = 70 [km/h]	V = 200 [km/h]
Crust	1.1	1500	72	65	500	500
Organic clay	3.0	1260	41	33	500	500
Clay	4.5	1475	65	60	1500	1500
Clay	6.0	1475	87	85	1500	1500
Half-space	–	1475	100	100	1500	1500

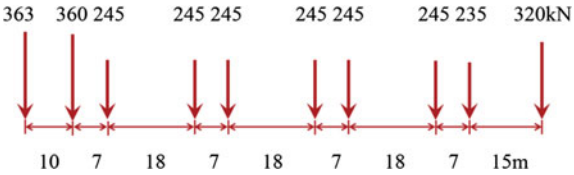

Fig. 6.3 Bogie loads of X-2000

is quasi-static, while those at the critical speed and trans-seismic conditions are dynamic. The latter are characterized by upward and downward oscillations and considerably larger amplitudes. The relatively low critical speed (around 200 km/h) is primarily due to the soft peat layer at about 1.5 m depth. If this layer is replaced by, for example, sand/gravel or if it is stiffened by lime–cement columns, the Rayleigh wave velocity and critical speed will increase accordingly.

6.4 Measures to Increase Critical Speed

This section presents the results for effect of different countermeasures. Three cases were considered for this purpose: (1) stiffened track where the stiffness of the track is increased by for example improving the stiffness of the embankment or by placing a stiff girder under the track, (2) soil improvement under the track by for example replacing the natural soil with stiffer materials (Fig. 6.1c) and (3) use of piles under the track, namely piled track (Fig. 6.2). In each case, the time histories of the track displacements for the same train load (Fig. 6.3) were computed and compared with the displacements of the base case shown in Fig. 6.4.

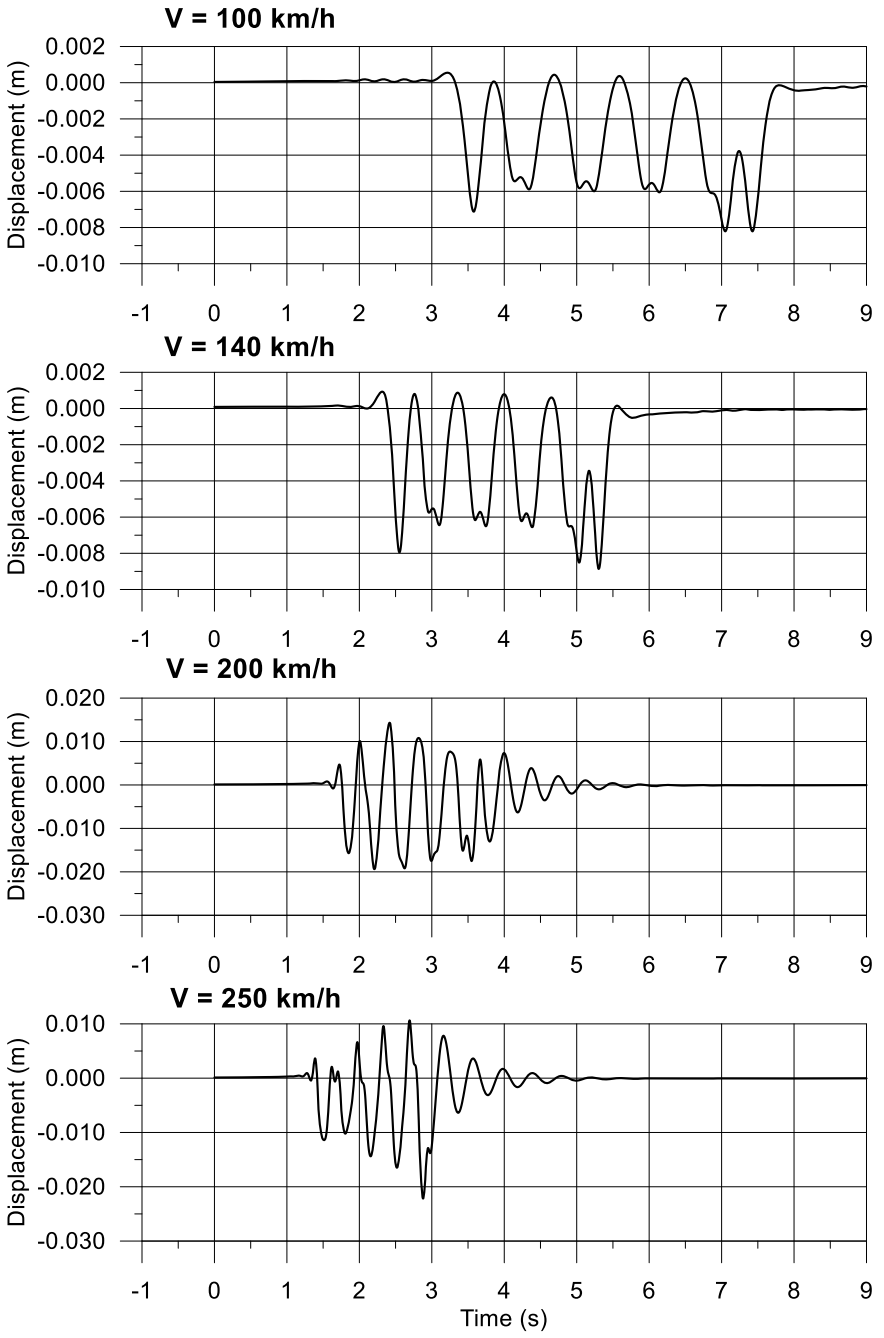

Fig. 6.4 Track displacements for low and high train speeds with track/ground model at Ledsgård

6.4.1 Track Stiffening

It is intuitive to think that stiffening the track, by for example use of a girder beam under the track, would reduce the vibrations and improve the performance of surface tracks. Figure 6.5 displays the track displacements for a case in which the total bending rigidity of the track is increased by a factor of 4 (to include a girder beam). Comparison of these results with those for the track in Fig. 6.4 indicates a considerable reduction of the response; however, the displacement oscillations for the speed 250 km/h indicates that the system is still in a trans-seismic regime. This is an undesirable condition for the track and should be avoided. While this measure is cable of reducing the track displacements, it will hardly affect the critical speed. To elucidate this point, Fig. 6.6 compares the trackside ground response for the base case and for the stiffened track for load speed 250 km/h. The figure demonstrates that the trackside vibration is only marginally reduced by stiffening the track, confirming the conclusion that track stiffening does not noticeably affect the critical speed although it could reduce the track response.

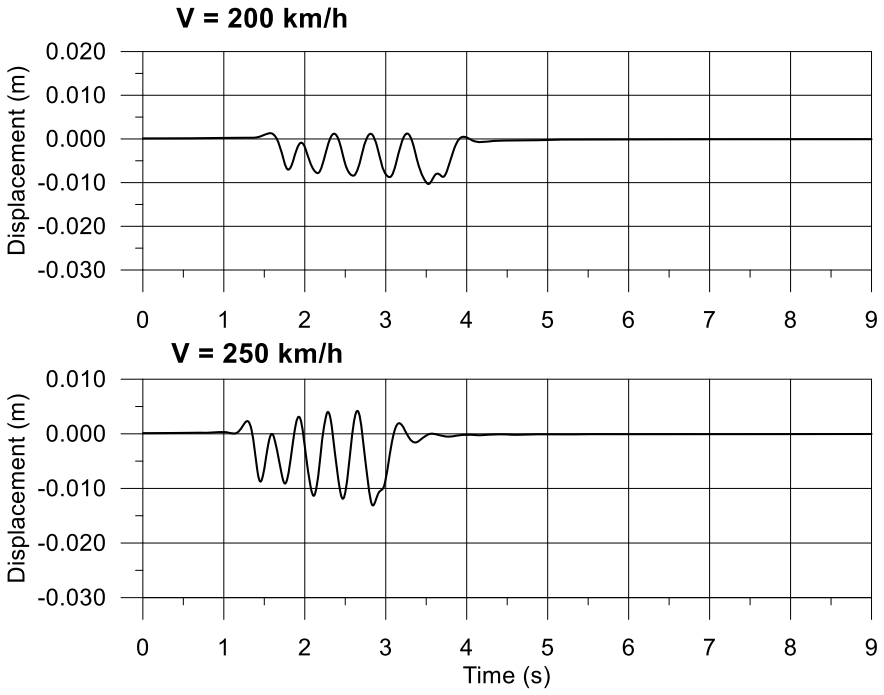

Fig. 6.5 Track displacements' track response under high train speeds for stiffened track

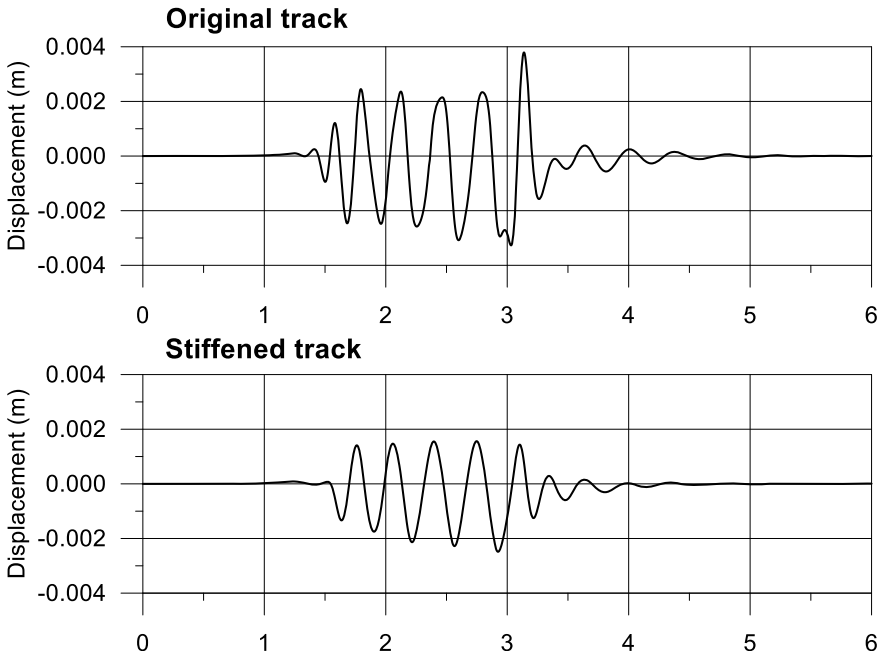

Fig. 6.6 Trackside ground displacements at 10 m distance for base case track (top) and stiffened track (bottom)

6.4.2 Ground Improvement and Soil Replacement

An effective solution for increasing the critical speed is stiffening the ground by either soil replacement or improvement techniques such as grouting or use of lime–cement columns (Norén-Cosgriff et al. 2019; Peplow and Kaynia 2007). Soil replacement is generally considered an expensive solution; however, it has the advantage that the properties of the new material are often more accurately known.

To assess the performance of ground improvement, the soil in the top two layers at Ledsgård site (Table 6.1) directly under the track was numerically replaced by gravel or crushed rock. It was assumed that the new material has an average shear wave velocity of 200 m/s. Moreover, for comparative purposes, the soil parameters of the track and the other soil layers were kept the same as in the base case. It should be noticed that this is strictly not correct because the soil parameters were selected by proper accounting for soil nonlinearity due to the induced stresses in the track and soil layers. The track response was then computed for the same loads (Fig. 6.3) using *VibTrain*.

The results of the numerical simulations are presented in Fig. 6.7. The plots in this figure clearly demonstrate that, although the track displacement increases with the train speed as expected, the responses for all the considered train speeds (in the

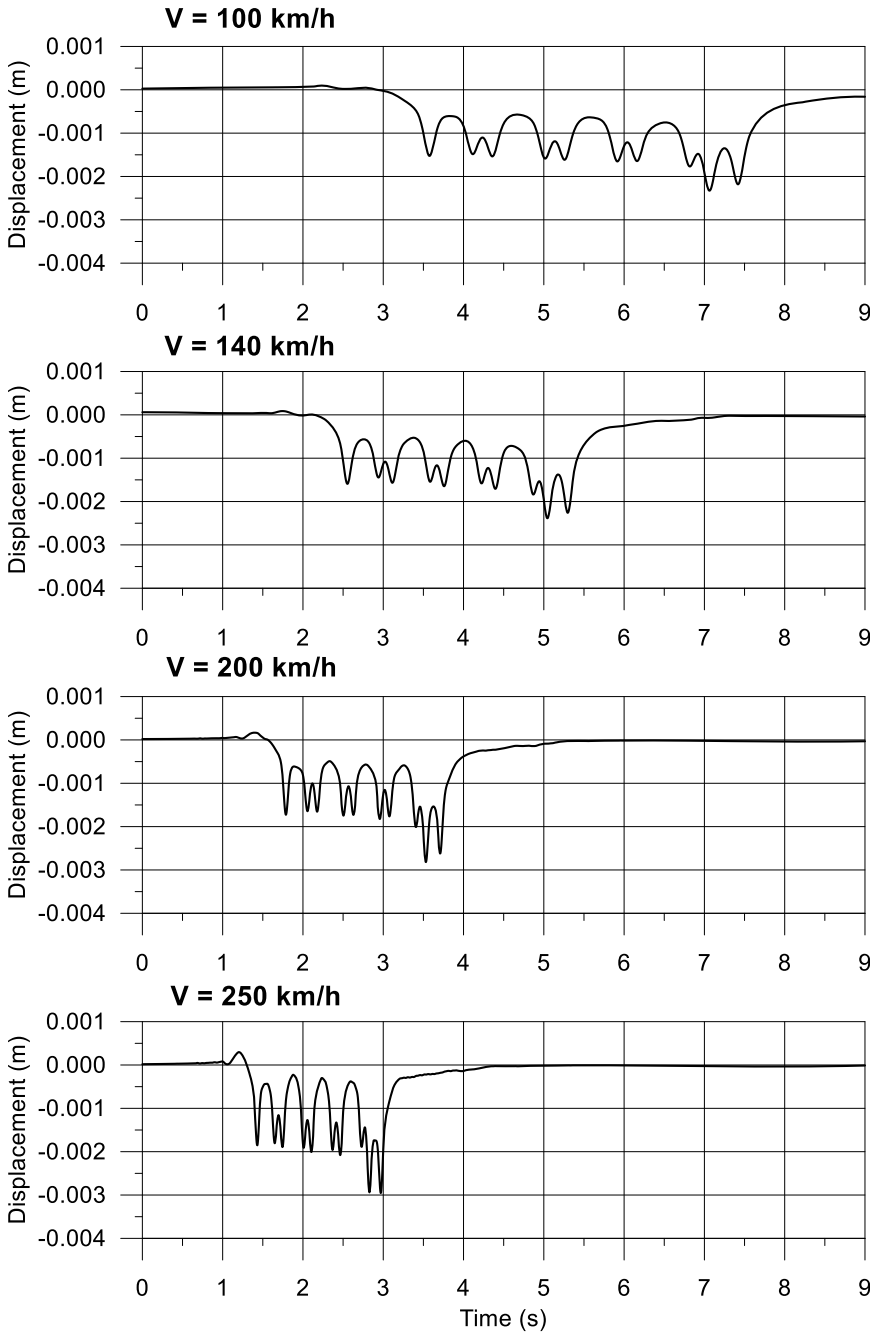

Fig. 6.7 Track displacements for low and high train speeds for soil replacement

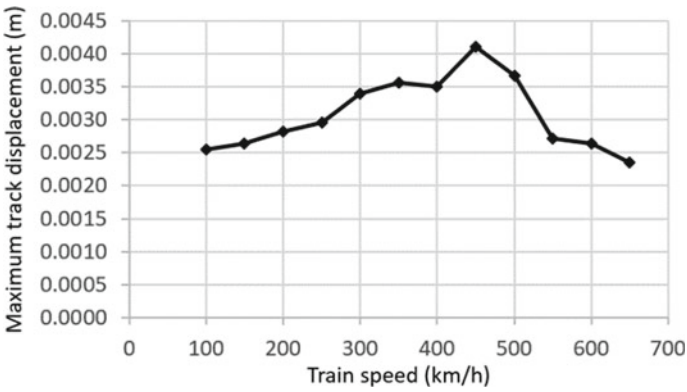

Fig. 6.8 Track displacements for low and high train speeds for soil replacement

range 100–250 km/h) are in the sub-seismic regime; that is, the responses are primarily quasi-static. These results confirm that soil replacement or ground improvement is a viable solution for increasing the critical speed.

For the above modified ground conditions, the critical speed was estimated by computing the maximum displacements of the track for increased train speed. Figure 6.8 shows a plot for the maximum track displacement as a function of the train speed in the range 100–700 km/h. The figure displays a peak displacement at a train speed of about 450 km/h. Therefore, the applied ground improvement has more than doubled the critical speed and has considerably reduced the displacements.

6.4.3 Piled Track

Another effective technique to reduce the critical speed is by use of piles under the track (Fig. 6.2). Piles have two functions in this regard. Firstly, they transfer the loads to deeper strata that are normally stiffer and hence contribute to generally stiffer track behavior. Secondly, the waves in the ground set up by one pile, as the load passes over the pile, do not excite the adjacent piles by the same extent as surface waves on the ground do. This is an important mechanism that leads to large track response when the load speed reaches the wave propagation velocity in the ground.

To investigate the performance of piled tracks, the same bending rigidity of the track in the stiffened track cased (Sect. 4.1) was used for the girder on the piles. The piles were assumed to have a diameter of 2 m and installed to the bottom of the third layer (i.e., about 9 m long, see Table 6.1). The spacing of the piles was taken as 12.0 m.

Figure 6.9 presents the results of simulations for the track response for the train speeds in the range 140–250 km/h. The plots show the time histories of the displacements for a section directly over the piles. The corresponding results for the mid-sections of the girder are displayed in Fig. 6.10. Comparing these results with those for the stiffened track on ground surface for the same speeds (Fig. 6.5), one can observe that while the track responses over the piles are lower, the response of the mid-sections is significantly higher. This large response is due to the vibration of the girder between the piles, which as the plots indicate, is amplified as the load speed increases.

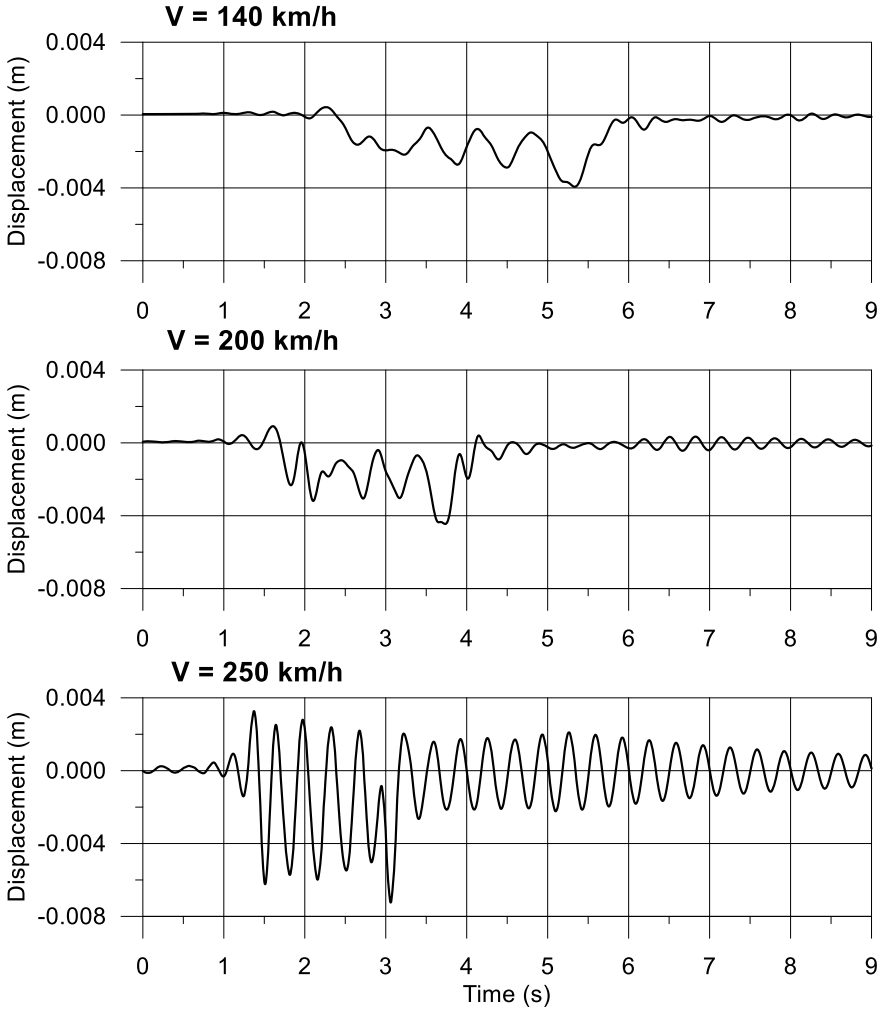

Fig. 6.9 Response of piled track at pile locations for low and high train speeds

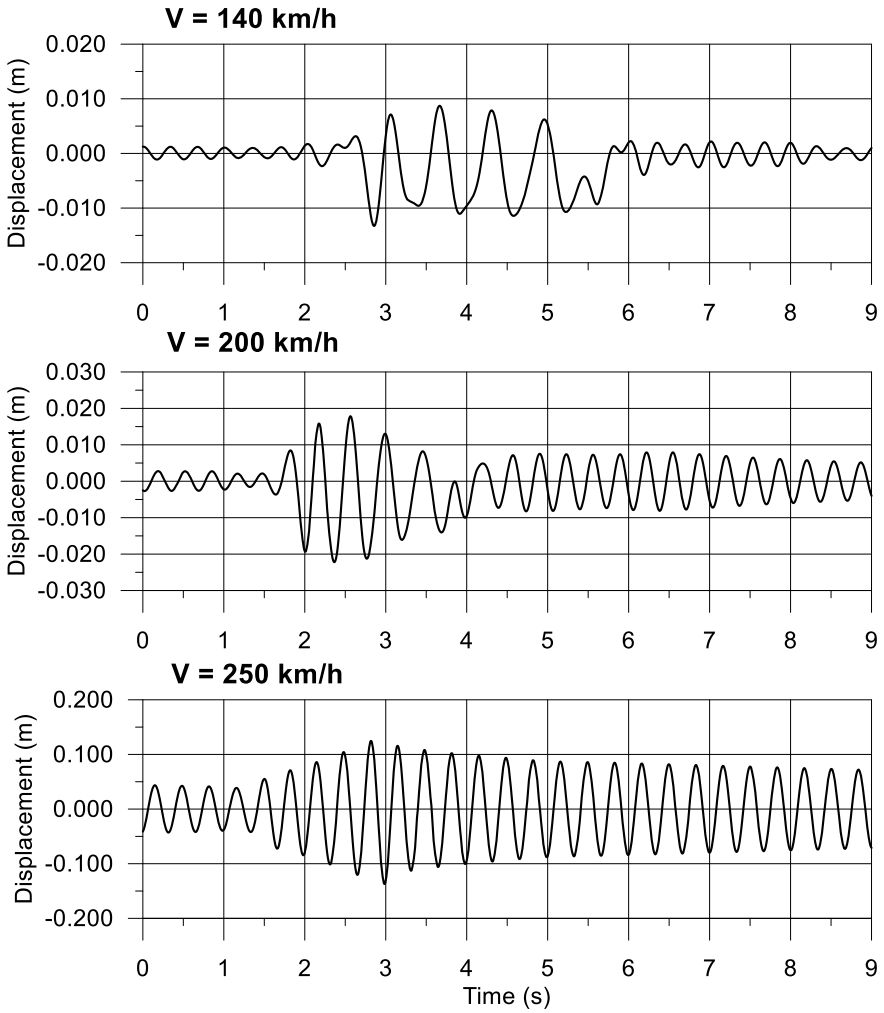

Fig. 6.10 Response of piled track at mid-section of girders for low and high train speeds

The results presented in this section indicate that while piled tracks could increase the critical speed and reduce the track response, one needs to perform sensitivity analyses on the bending rigidity of the girder to ensure acceptable vibration at mid-spans. The design challenge has therefore been moved from the critical speed issue to the proper structural design of the girder.

6.5 Conclusion

This paper presented an overview of the developments in the subject of moving loads over layered ground. Two analytical–numerical models based on the use of Green's functions in viscoelastic layered ground were presented. The first model is for conventional tracks on ground surface, and the second model is for elevated tracks on girders supported by piles. Typical results of simulations for both models were presented, and the responses in the speed regimes sub-seismic and trans-seismic were discussed. It was shown that one can reduce the track vibration near the critical speed by stiffening the track although not being able to noticeably alter the critical speed. Moreover, the trackside ground surface vibration is not significantly reduced.

Use of piles under tracks, namely piled tracks, appears to increase the critical speed; however, special attention should be given to design of the girders to avoid excessive track vibration between the piles.

Ground improvement or soil replacement under the track was shown to be a reliable solution for increasing the critical speed; however, it should be noticed that soil replacement is often a costly operation. Ground improvement techniques such as use of lime–cement columns could offer more economical alternatives.

References

Achenbach JD, Keshava SP, Herrmann G (1967) Moving load on a plate resting on an elastic half space. J Appl Mech 34:910–914

Andersen L, Jones CJC (2006) Coupled boundary and finite element analysis of vibration from railway tunnels—a comparison of two- and three-dimensional models. J Sound Vib 293:611–625

Ang DD (1960) Transient motion of a line load on the surface of an elastic half-space. Quart Appl Math 18:251–256

Aubry I, Clouteau D, Bonnet G (1994) Modeling of wave propagation due to fixed or mobile dynamic sources. In: Proceedings of workshop Wave'94, Ruhr University, Berg-Verlag, Bochum, pp 79–93

Auersch L (2005) The excitation of ground vibration by rail traffic: theory of vehicle-track-soil interaction and measurements on high-speed lines. J Sound Vib 284:103–132

Baron ML, Bleich HH, Wright JP (1967) Ground shock due to Rayleigh waves from sonic booms. J Engng Mech Div ASCE 93(5):135–162

Cole J, Huth J (1958) Stress produced in a half-space by moving loads. J Appl Mech 25:433–436

Coulier P, Francois S, Degrande G, Lombaert G (2013) Subgrade stiffening next to the track as a wave impeding barrier for railway induced vibrations. Soil Dyn Earthq Eng 48:119–131

Craggs JW (1960) Two-dimensional waves in an elastic half-space. Proc Cambridge Phil Society 56:269–275

de Barros FCP, Luco JE (1994) Response of a layered viscoelastic half-space to a moving point load. Wave Motion 19:189–210

Eringen AC, Suhubi ES (1975) Elastodynamics, volume II: linear theory. Academic Press, Inc., New York

Filon LNG (1928) On a quadrature formula for trigonometric integrals. Proc Roy Soc Edinburgh 49:38–47
Frýba L (1973) Vibration of solids and structures under moving loads. Noordhoff International Publishing, The Netherlands
Hall L (2003) Simulations and analyses of train-induced ground vibrations in finite element models. Soil Dyn Earthquake Eng 23:403–413
Karlström A, Boström A (2006) An analytical model for train induced ground vibrations from railways. J Sound Vib 292:221–241
Kausel E, Roesset JM (1981) Stiffness matrices for layered soils. Bull Seism Soc Am 71(6):1743–1761
Kaynia AM (1988) Characteristics of the dynamic response of pile groups in homogeneous and nonhomogeneous media. In: Proceedings 9th world conference earthquake engineering, vol 3, Tokyo-Kyoto, Japan, pp 575–580
Kaynia AM (2001) Measurement and prediction of ground vibration from railway traffic. In: Proceedings of the 15th international conference on soil mechanics and geotechnical engineering, vol 3. Istanbul, Turkey, 27–31 Aug, pp 2105–2109
Kaynia AM, Kausel E (1991) Dynamics of piles and pile groups in layered soil media. Soil Dyn Earthquake Eng 10(8):386–401
Kaynia AM, Madshus C, Zackrisson P (2000) Ground vibration from high-speed trains: prediction and countermeasure. J Geotech Geoenviron Eng 126(6):531–537
Kaynia AM, Park J, Norén-Cosgriff K (2017) Effect of track defects on vibration from high speed train. Proc Eng 199:2681–2686
Krylov VV (1995) Generations of ground vibrations from superfast trains. Appl Acoustics 44:149–164
Madshus C, Kaynia AM (2000) High-speed railway lines on soft ground: dynamic behaviour at critical train speed. J Sound Vibration 231(3):689–701
Niwa Y, Kobayashi S (1966) Stresses produced in an elastic half-space by moving loads along its surface. Mem Fac Engng Kyoto Univ 28:254–276
Norén-Cosgriff KM, Bjørnaråa TI, Dahl BM, Kaynia AM (2019) Advantages and limitation of using 2-D FE modelling for assessment of effect of mitigation measures for railway vibrations. Appl Acoust 155:463–476
Pan G, Atluri SN (1995) Dynamic response of finite sized elastic runways subjected to moving loads: a coupled BEM/FEM approach. Int J Num Meth Eng 38:3143–3166
Papadopoulos M (1963) The elastodynamics of moving loads. J Australian Math Soc 3:9–92
Park J, Kaynia AM (2018) Stiffness matrices for fluid and anisotropic soil layers with applications in soil dynamics. Soil Dyn Earthq Eng 115:169–182
Payton RG (1964) An application of the dynamic Betti-Rayleigh reciprocal theorem to moving point load in elastic media. Quart Appl Math 21:299–313
Peplow A, Kaynia AM (2007) Prediction and validation of traffic vibration reduction due to cement column stabilization. Soil Dyn Earthq Eng 27:793–802
Sackman JL (1961) Uniformly moving load on a layered half-plane. J Eng Mech Div ASCE 87 (4):75–89
Sneddon IN (1951) Fourier transforms. McGraw-Hill Book Company, New York
Wright JP, Baron ML (1970) Exponentially decaying pressure pulse moving with constant velocity on the surface of a layered elastic material (superseismic layer, subseismic half-space). J Appl Mech 96:141–152